Torque-winding interdependence for a flexible polymer chain wound around a cylinder in the presence of obstacles

Boris P. Belotserkovskii

Phys. Rev. E **93**, 032509 — Published 30 March 2016

DOI: 10.1103/PhysRevE.93.032509

Torque-winding interdependence for a flexible polymer chain wound around a cylinder in the presence of obstacles.

Boris P. Belotserkovskii

Department of Biology, Stanford University

371 Serra Mall, Herrin Labs, Stanford, CA 94305-5020

e-mail: borisbp@stanford.edu

phone: (650)-723-2425

fax: (650)-725-1848

ABSTRACT

Polymer chains winding around each other, or around other objects occur in many natural systems; the physical consequences of this winding are therefore of significant interest. A polymer chain could be surrounded by various bulky objects (further referred as "obstacles"), such as other macromolecules or macromolecular aggregates. Here we show that for a long flexible polymer chain wound around a cylinder, the presence of obstacles could modify the winding-torque interdependence, in some cases leading to phase transition-like behavior, in which the winding occurs only when the torque exceeds some critical value. Possible implications of this effect are discussed in relation to the biophysics of nucleic acids.

I. INTRODUCTION

Properties of polymer chains that are wound around each other, or around other objects are of significant interest and have been broadly studied ([1, 2] and references therein). Of particular interest is interdependence between the winding and the torque [3-5]. We recently analyzed a torque-winding interdependence for very long ideal polymer wound around a cylinder (Fig.1A, left) [3]. We found that the character of this dependence is different for small and for large torques: For small torques, the dependence is non-linear, while for large torques the dependence obeys a linear Hooke's law. That difference in behavior arises because the tangential chain stretching required for a given degree of winding increases with the distance between the chain and the axis of the cylinder (Fig.1A, right); consequently, the farther the chain from the axis of the cylinder the greater its resistance against winding. At small torques, the characteristic distance between the axis of the cylinder and the chain is large, and, consequently, the chain's resistance against winding is also large. Upon increase in torque, the winding of the chain around the cylinder increases, which brings the chain closer to the cylinder, thus decreasing the chain's resistance against winding. This decrease in the resistance against winding upon increase in torque results in non-linearity of torque-winding interdependence; and it also causes non-linear interdependence between the torque and the angular velocity for a polymer chain rotating in viscous media [3, 6, 7]. Eventually, upon further increase in torque, the distance between the chain and the axis of the cylinder approaches a constant value equivalent to the radius of the cylinder. Consequently, the chain's resistance against winding ceases to depend upon the torque,

and the torque-winding interdependence becomes linear. It is important to note that this switching between the regimes occurs smoothly, without phase transition-like behavior.

A flexible polymer chain wound around a cylinder could serve as simplified model for intertwined biopolymers. For example, we have used this model to estimate mechanical stress in RNA and DNA during transcription that appears when the relative rotation of the nascent RNA and DNA is constrained, to result in RNA winding around DNA [3, 8].

In the previously considered model [3], the only region in space impenetrable for the polymer chain was those occupied by the cylinder. In many real situations (e.g. in a living cell), any given macromolecule (e.g. transcribed DNA segment) is surrounded by other impenetrable objects (e.g. macromolecules or macromolecular aggregates). Thus, it is of interest to analyze the effect of including of such objects (further referred as "obstacles") upon polymer chain winding.

In this work, we will consider two types of obstacles, which we will refer to as "topological" and "non-topological".

A topological obstacle could be visualized as an infinitely long rod, which is not interlinked with the chain (Fig.1B, left; in our simplified model, we will assume that the rod is parallel to the cylinder)). If the chain, upon winding around the cylinder, encounters such an obstacle, it cannot go all the way around it, i.e. if the chain protrudes around the obstacle, it must retrace its way back (Fig. 1B, right). This retracing would cancel winding around the cylinder within the respective region of the chain. Of course, such a retracing occurs randomly within some regions of the chain even without topological obstacles; however, the obstacle(s) would force upon the chain "obligatory"

retracing, which would decrease the propensity of the chain to wind around a cylinder. For example, for a region of the chain protruded in between two topological obstacles, the winding angle cannot exceed the angle between the vectors connecting the obstacles and the axis of the cylinder (Fig.2). (An important special case is when the obstacles and the center of the cylinder are lying on the same line; in this case the winding angle of the loop protruded beyond this line is exactly zero.) Upon increase in winding, the chain is pulled closer to the cylinder, which causes "shrinking" of the chain's regions that are protruding around or between topological obstacles, and, consequently, compliance of the chain towards winding increases. Thus, the presence of topological obstacles additionally contributes to positive feedback between the winding and the compliance to winding. Because of that, one can expect that in the presence of topological obstacles the winding-torque interdependence would exhibit a "sharper" switching between regimes upon increase in torque than in the absence of topological obstacles.

The presence of multiple topological obstacles increases the difference in compliance to torque between the regions of the chain localized far from the cylinder, which are more likely to be localized within loops protruded between the obstacles (and thus have strongly diminished ability to wind), and the regions localized in the vicinity of the cylinder, which are more likely to have "non-compromised" winding ability. In this paper we argue that this contrast between the proximal and distal regions of the chain creates a formal similarity between the chain winding around the cylinder and the chain adsorption on a solid surface, which is known to exhibit phase transition-like behavior (reviewed in [9]).

Non-topological obstacles (Fig.1C) could be visualized as relatively small compact objects, which occupy some volume in space, making it unavailable for the chain. We will show that in contrast to the topological obstacles, non-topological obstacles affect torque-winding interdependence only if their concentration changes with the distance from the cylinder, and some profiles of the obstacle concentrations could lead to phase-transition-like behavior of the torque-winding interdependence.

Thus, in general, the presence of obstacles could produce significant effects on the behavior of a wound polymer chain, as we have analyzed in this paper.

II. RESULTS

A. Overview of the results for the chain in the absence of obstacles.

Here we repeat (with some additional analysis) the derivation and briefly summarize the results previously reported for the model in the absence of obstacles [3] that we are going to use in the further analysis.

In the continuous approximation, the statistical weight W of the Gaussian chain comprising N segments is described by the diffusion-like equation

$$\frac{\partial W}{\partial N} = \frac{l^2}{2}\nabla^2 W \tag{1}$$

Here l is the length of the chain segments divided by square root from the system dimensionality (e.g. by $\sqrt{3}$ in the case of three-dimensions).

Because the Gaussian chain deformations in different directions are independent, and we are interested only in the chain winding, we can consider a two-dimensional version of Eq. 1 in the polar coordinates:

$$\frac{\partial W}{\partial N} = \frac{l^2}{2}\left(\frac{\partial^2 W}{\partial r^2} + \frac{1}{r}\frac{\partial W}{\partial r} + \frac{1}{r^2}\frac{\partial^2 W}{\partial \phi^2} \right) \tag{2}$$

where r is the distance from the cylinder axis, and ϕ is the winding angle around this axis.

If a constant torque M is applied to the chain, then the partial function of the chain is

$$W_M = \int_{-\infty}^{+\infty} W \exp\left(\frac{M\phi}{kT} \right) d\phi \tag{3}$$

Multiplying Eq.2 by $\exp\left(\frac{M\phi}{kT} \right)$ and integrating over $-\infty < \phi < +\infty$, we obtain:

$$\frac{\partial W_M}{\partial N} = \frac{l^2}{2}\left(\frac{\partial^2 W_M}{\partial r^2} + \frac{1}{r}\frac{\partial W_M}{\partial r} + \frac{\left(\frac{M}{kT}\right)^2}{r^2} W_M \right) \tag{4}$$

We will look for a solution of Eq.4 as a linear combination of the functions with factorized spatial and length dependences of the general form:

$$\psi(N,r) = g(r)\exp(\varepsilon N) \tag{5}$$

where ε is some dimensionless parameter.

Substituting Eq.5 into Eq.4, and introducing dimensionless coordinate

$$x \equiv r\frac{\sqrt{2\varepsilon}}{l} \tag{6}$$

and normalized torque

$$q \equiv \frac{M}{kT} \tag{7}$$

we obtain:

$$x^2\frac{d^2g}{dx^2} + x\frac{dg}{dx} + \left(q^2 - x^2\right)g = 0 \tag{8}$$

This is a modified Bessel equation of purely imaginary order iq.

The function $g(x)$ is proportional to the probability for the end of the chain to be at the coordinate x. Thus, its integral over the whole space available for the chain (in this case,

from the surface of the cylinder to infinity) must converge. The solution of Eq.8 that can satisfy this requirement is the modified Bessel function of the second kind (also known as the modified Hankel function, the modified Bessel function of the third kind and some other designations) of purely imaginary order $K_{iq}(x)$([10] and references therein). This function has infinite number of positive roots, which values depend upon parameter q. Importantly, there is the *largest* root, usually designated x_1. At $x > x_1$, the function remains positive, first reaching a local maximum, and then monotonically decreasing, approximately as $e^{-x}/x^{1/2}$. At $x < x_1$ the function is oscillating between the positive and negative values, with frequency indefinitely increasing upon approaching $x = 0$, producing infinite sequence of roots $x_2, x_3, x_4 \ldots$, which values approaching zero upon increasing in the root's number.

Because within the continuous approximation, the partial function of the chain must be zero at an impenetrable surface, the surface of the cylinder (i.e. $r = R$, where R is the radius of the cylinder), must correspond to one of the roots of the function $K_{iq}(x)$. (Note that in the original formulation of the problem, we consider the end(s) of the chain attached to the surface of the cylinder (e.g. Fig.1A; left). However, when we use a continuous approximation, we have to re-define the attachment as positioning at some small, but finite (e.g. about the length of one segment) distance from the surface, because within the continuous approximation, the partial function (and thus, the probability of localization for any segment of the chain) on the surface of the cylinder is zero. That wouldn't affect significantly the results, especially for long chains, for which precise ends positions are not important.)

Solution of Eq.8, in which the root number m (i.e. x_m) corresponds to the surface of the cylinder is

$$g_m(r) = K_{iq}\left(r\frac{x_m}{R}\right) \tag{9}$$

(Here we have expressed g as a function of r instead of x, using the fact that r is proportional to x (Eq.6), and that if $r = R$, then $x = x_m$.)

From Eq.6 and the condition that if $r = R$, then $x = x_m$, the parameter ε that corresponds to the solution given by Eq.9 is

$$\varepsilon_m = x_m^2\frac{l^2}{2R^2} \tag{10}$$

Substituting this result into Eq.5, we obtain:

$$\psi_m(N,r) = g_m(r)\exp\left(x_m^2\frac{l^2}{2R^2}N\right) = K_{iq}\left(r\frac{x_m}{R}\right)\exp\left(x_m^2\frac{l^2}{2R^2}N\right) \tag{11}$$

The functions from Eq.11 that correspond to different values of m comprise an orthogonal set at the interval $R < r < \infty$, and, in general, using their linear combination, we can obtain solution for any initial conditions (i.e. precise position, or positions distribution for the start of the chain). However, from Eq.11 it is seen that the term that corresponds to the largest root x_1 becomes increasingly predominating upon growing of

the chain length, and for sufficiently long chains all other terms could be neglected, thus we obtain partial function with factorized length and space dependences:

$$W_M(N,r) \sim \psi_1(N,r) \equiv g_1(r) \exp\left(x_1^2 \frac{l^2}{2R^2} N \right) \tag{12}$$

The physical meaning of the solution with factorized spatial and length dependences (Eq.12) is that for very long chains, the distribution of the segments positions relative to the cylinder practically doesn't depend upon the length of the chain, and upon the initial conditions. For these very long chains, N-dependent exponential term in Eq.12 practically defines all parameters of the chain; and the free energy of the chain is proportional to N. The solution with factorized spatial and length dependences given by Eq.12 is possible due to the presence of torque, which, by facilitating the chain winding around the cylinder, creates an apparent force that brings the chain closer to the cylinder. In the absence of torque, the characteristic distance between the chain and the cylinder will grow indefinitely with the chain length, and, consequently, the solution with factorized spatial and length dependences is not applicable. In general, solution with factorized spatial and length dependences could be realized for the chain localized in some compressing field (e.g., in the simplest case, when the chain is confined in a cavity), but is not applicable for a free chain (reviewed in [11]).

As we already mentioned (see the text below Eq.8), the roots of the function $K_{iq}(x)$ depend upon the parameter q (which is the order (times $-i$) of the function $K_{iq}(x)$, and is equivalent to the normalized torque (Eq.7)). As we have shown previously [3], for a

very long ideal polymer chain which partial function is described by Eq.12, physical parameters of the chain can be obtained from the dependence of the largest root x_1 of the function $K_{iq}(x)$ upon the parameter q. In particular, the winding angle per one segment is

$$u = \frac{1}{2}\left(\frac{l}{R}\right)^2 \frac{d\left(x_1^{\,2}\right)}{dq} \tag{13}$$

The parameter

$$r_b = \frac{R}{x_1} \tag{14}$$

defines the characteristic size of the chain's region at which the conformation of the region switches from the coil weakly perturbed by torque (i.e. the amplitude of perturbation induced by torque is smaller that the amplitude of random thermal fluctuations) to strongly perturbed coil. This characteristic size is an analog of the tensile blob size in the stretched polymer chain [12], and, from this analogy, it has been termed the "torsional blob" size [3]. If this size is much larger than the radius of the cylinder, it could be interpreted as a characteristic distance between the chain and the cylinder.
The free energy of the chain comprising N segments is

$$\Delta G = -NkT\frac{l^2}{R^2}\frac{x_1^2}{2} = -kT\frac{N}{2\left(r_b/l\right)^2} \tag{15}$$

The dependence $x_1(q)$ is positive, strictly increasing (except the point $q = 0$ at which $x_1(q)$ and all its derivatives approach zero) continuous smooth function of q. A general analytical expression for the function $x_1(q)$ is not known, although numerical results for its estimation, as well as asymptotics are available [10].

In particular, for small q:

$$x_1(q) \approx \exp\left(-\frac{\pi}{q}\right) \tag{16}$$

and for large q:

$$x_1(q) \approx q \tag{17}$$

For further analysis, we are interested in the properties of the chain under the torque, that is confined in a certain region of space with a characteristic size λ.

If λ is larger than the size of the torsional blob (Eq.14), then the chain wouldn't "notice" the confinement, and the free energy of the chain would be given by Eq.15.

If λ is smaller than the size of torsional blob, than the chain could be considered as comprised of virtually unperturbed coils of the size λ containing

$$n_\lambda \sim \left(\frac{\lambda}{l}\right)^2 \tag{18}$$

segments.

Because the size of these coils is smaller then the size of torsional blob, and consequently, their shapes are weakly perturbed by the torque, for each of these coils the torque-induced directed winding angle ϕ_λ is smaller than the amplitude of the symmetric thermal fluctuations $\phi_{\lambda T}$ of the winding angle in the absence of torque. Thus, ϕ_λ could be viewed as small perturbation of the shape of the coil; and, consequently, the free energy of the coil at a given value of ϕ_λ could be approximated by its Taylor expansion up to quadratic terms:

$$\Delta G_{\phi_\lambda}(\phi_\lambda) = kT\left(\frac{1}{2}\left(\frac{\phi_\lambda}{\phi_{\lambda T}}\right)^2 - q\phi_\lambda\right) \tag{19}$$

Within this approximation, ϕ_λ has Gaussian distribution, and consequently the free energy of the coil ΔG_λ at given torque averaged over all possible values of ϕ_λ corresponds to the minimum of the Eq.19:

$$\Delta G_\lambda(q) = kT\ \min\left(\frac{1}{2}\left(\frac{\phi_\lambda}{\phi_{\lambda T}}\right)^2 - q\phi_\lambda\right) = -\frac{kT}{2}\left(q\phi_{\lambda T}\right)^2 \tag{20}$$

which occurs at

$$\phi_{\lambda(\min)} = \langle \phi_\lambda \rangle = q\,\phi_{\lambda T}^2 \tag{21}$$

(Here brackets $\langle\ \rangle$ designate average over all configurations, which in the case of Gaussian distribution is equivalent to the value that corresponds to the minimum of the free energy.) Note that in Eq.20, as well as in Eq.15, the zero level of the free energy corresponds to the zero torque.

The amplitude of the thermal fluctuation of the winding angle for unperturbed ideal coil is related to the number of the segments within the coil (Eq.18) as:

$$\phi_{\lambda T} \sim \ln n_\lambda = \ln\left(\frac{\lambda}{l}\right)^2 \tag{22}$$

(see [2, 13] and references therein)

Combining Eqs 20 and 22, we obtain

$$\Delta G_\lambda(q) \sim -kT\left(q \ln\frac{\lambda}{l}\right)^2 \tag{23}$$

B. Torque-winding interdependence in the array of topological obstacles.

Consider an ideal chain in an array of obstacles that creates a grid of "cages", with the cylinder localized in the middle of the central cage (Fig.3A).

It is seen that for chain regions localized in the central cage the winding capabilities are unrestricted, while for the regions outside the central cage the winding capabilities are limited, and these limitations become stronger upon increasing the distance from the central cage. For example, from simple geometrical considerations (similar to ones in Fig.2), it can be obtained that for the regions protruded from the central cage the maximal achievable winding angle is $\pi/2$; for the regions protruded from the cages localized farther from the center, the maximal winding angle decreases further. Moreover, for the loops "cut out" by imaginary rays emanating from the center of the cylinder (an example of such a ray is shown in Fig.3A by a dotted line), the winding angle would be exactly zero. For a sufficiently long chain, most of the chain's segments belonging to the regions expanded into the grid would be within such zero-winding loops. Based upon these considerations, we suggest a simplified model, in which we neglect the contribution to the winding from the regions outside the central cage, postulating that only the regions inside the central cage are capable to wind, and, consequently are "responsive" to torque. This means that, within this approximation, in each cage, except the central one, the confined region of the chain doesn't experience any external forces and consequently, behaves like an unperturbed coil comprising $n_\lambda \sim (\lambda/l)^2$ segments. Based upon that, we will represent the polymer chain as consisting of "supersegments", of which each is confined within a single cage, and contains n_λ actual segments. These supersegments are not affected by torque, except those that are localized in the central cage containing the cylinder (Fig.3A), where, in response to torque, they are able to wind around the cylinder.

The free energy of a supersegment within the central cage is given either by Eqs.20, 23, or Eq.15 (the latter with replacement of n_λ for N), depending upon whether the size of the torsional blob is larger or smaller than the size of the cage, respectively. This free energy could be interpreted as an energy of "adsorption" of the supersegment in the central cage. (Here we want to emphasize that in our model "adsorption" means localisation of the supersegment in the central cage containing the cylinder. The spatial distribution of the segments within the adsorbed supersegment depends upon the torque, and, in general, they need not to be in close contact with the cylinder, like in the case of "real" adsorption on the cylinder's surface.)

Thus, as a basic model (Fig.3B) we approximate the chain as a random walk trajectory (with an apparent number of steps $\mathrm{N} = N / n_\lambda$) on the grid created by obstacles, with reversible adsorption in the central cell. Since the ends of the chain are attached to the cylinder, this trajectory begins and ends in the central cage; and we also require that the chain is not linked to any of obstacles.

Such a closed chain in the array of obstacles (with which it is not linked) could be mapped into a random walk trajectory along a Cayley tree (Fig.3C) (for review see [11, 14]). Within this tree, the branching points (nodes) are localized in the middle of the cage, the number of branches κ emanating from each branching point is equivalent to the number of immediate neighboring cages for a cage within a grid (for example, for the two-dimensional grid shown in Fig.3B, $\kappa = 4$). Nodes of the same generation (X) comprise a "shell", which will be referred to as "the shell number X" (Fig.3C).

The rational for using the Cayley tree representation is that the number of possible trajectories formed by the closed chain embedded into an array of obstacles (with which

it is not linked) is the same as the number of possible trajectories of the same length formed by a particle that walks randomly along the branches of the tree, and at the end returns to the origin from which it started its walk (for review see [11, 14]). As an example, Fig.3C shows "tree-representation" for the trajectory from the Fig.3B.

This approach allows one to reduce the calculation of the partial function for the chain of interest to a one-dimensional random walk problem, using the shell's number (X) as a coordinate to describe the position of the "walker" (Fig.4). In the framework of this description, returning to the origin (which in our case is in the central cage) corresponds to positioning the end of the chain at $X = 0$. Note that this definition for return to the origin in terms of the tree-based model is consistent with the topological nature of "adsorption" in our system: in principle, the region of the chain localized within the tree at some position with $X \neq 0$, in real space can be localized within the central cage (it would correspond to a loop protruding into the central cage from the outside, as in the example shown in Fig.5). If we were dealing with usual adsorption (e.g. due to some electrostatic or hydrophobic interactions between the chain and the cylinder), we would consider this region as being adsorbed. However, because the chain region within this loop is not able to wind around a cylinder, in terms of our model it is not adsorbed, i.e. "topological" adsorption happens only when $X = 0$.

Our description of the random walk along the Cayley tree is similar to that in [15, 16], with the modification that at each step, "the walker", in addition to moving to the neighboring position, could also remain at the same position, as previously done for discrete random walk-based polymer adsorption models (e.g. [17]). (Note that the "same position" in this context means the same apparent coordinate. For example, in our case

remaining in the same position actually occurs in a 2D-projection perpendicular to the axis of the cylinder. In 3D-space, the segments could shift along the axis of the cylinder while their positions on 2D-projections remain the same. That doesn't make difference for an ideal chain, but should be taken into account if the model is extended to real chains with excluded volumes.)

Since in each node the "parental" branch is divided into $b = \kappa - 1$ branches, then at each node within the shell number X (except the origin $X = 0$) there are b ways to move to the shell $X+1$, and only one way either to move to the shell $X-1$, or to stay at the same place. From the origin ($X = 0$), there is $\kappa = b+1$ way to move to $X = 1$.

Thus, for the number of trajectories S comprising of N steps and ending in X we can write recurrence equations:

$$S(\mathrm{N}, X) = b\,S(\mathrm{N}-1, X-1) + S(\mathrm{N}-1, X) + S(\mathrm{N}-1, X+1); \quad X > 1 \tag{24}$$

$$S(\mathrm{N}, 1) = \kappa\,S(\mathrm{N}-1, 0) + S(\mathrm{N}-1, 1) + S(\mathrm{N}-1, 2) \tag{25}$$

$$S(N, 0) = S(\mathrm{N}-1, 0) + S(\mathrm{N}-1, 1) \tag{26}$$

(As would be seen below, during the derivations it is useful to keep κ and b as independent parameters without making the substitution $\kappa = b+1$. However, we always assume that $\kappa > b > 1$)

For all supersegments localized outside the central cage the free energy is the same and could be set as a zero level; thus, for these positions the recurrence equations for the

partial function of the chain Z would be the same as for the number of trajectories (Eqs. 24, 25). In the central cage (i.e. at $X = 0$), the supersegments have additional, torque-dependent component of free energy $\Delta G_\lambda(q)$, thus, to obtain the partial function for trajectories which end in the central cage $X = 0$, the number of trajectories the right half of the Eq.26 must be multiplied by a factor

$$\upsilon \equiv \exp\left(-\Delta G_\lambda / kT\right) \tag{27}$$

Thus, for partial function Z of the chain we obtain:

$$Z(\mathrm{N}, X) = b\,Z(\mathrm{N}-1, X-1) + Z(\mathrm{N}-1, X) + Z(\mathrm{N}-1, X+1); \quad X > 1 \tag{28}$$

$$Z(\mathrm{N}, 1) = \kappa\, Z(\mathrm{N}-1, 0) + Z(\mathrm{N}-1, 1) + Z(\mathrm{N}-1, 2) \tag{29}$$

$$Z(\mathrm{N}, 0) = \upsilon Z(\mathrm{N}-1, 0) + \upsilon Z(\mathrm{N}-1, 1) \tag{30}$$

We will consider a solution for this system that corresponds to a "homogeneous" configuration of a very long chain, where the distributions of positions of supersegments localized sufficiently far from the ends of the chain are the same and don't depend upon the chain length. In this case, the free energy of the chain would be proportional to the number of supersegments N. Consequently, partial function should be exponential upon N; thus we will be looking for solution in the form

$$Z(\mathrm{N},X)=a^{\mathrm{N}}f(X) \tag{31}$$

As we mentioned before (see the text below Eq.12), this type of solution could be realized for sufficiently long chains in the presence of some apparent attraction forces (in this case created by torque) acting upon the chain (or part of the chain) towards the origin.

In this case, the system of Eqs. 28-30 produces:

$$(a-1)f(X)=b\,f(X-1)+f(X+1);\quad X>1 \tag{32}$$

$$(a-1)f(1)=\kappa f(0)+f(2) \tag{33}$$

$$(a-\upsilon)f(0)=\upsilon f(1) \tag{34}$$

Eq.32 is discrete analog of linear differential equation with constant coefficients, which solution can be found in the form $f(X)=A^X$, where A is some positive constant. (Here we omitted normalizing constant, which is not important for our analysis). Because $\kappa \neq b$, there is discontinuity of solution in the origin, i.e. instead of $f(0)=1$, we would assume that $f(0)=B$, where B is some constant.

Thus

$$f(X) = A^X; \quad X \geq 1 \tag{35}$$

$$f(0) = B \tag{36}$$

and

$$Z(\mathrm{N}, x) = a^{\mathrm{N}} A^X; \quad X \geq 1 \tag{37}$$

$$Z(\mathrm{N}, 0) = a^{\mathrm{N}} B \tag{38}$$

By substituting Eqs. 35, 36 into Eqs. 32-34, we obtain

$$(a-1)A = b + A^2 \tag{39}$$

$$(a-1)A = \kappa B + A^2 \tag{40}$$

$$(a-\upsilon)B = \upsilon A \tag{41}$$

from which we can determine parameters A, B, and a.

However, we will first determine at which value of parameter A non-zero solution of the type given by Eqs. 37, 38 is possible for our boundary conditions, i.e. when both ends of the chain are localized in the origin. For that, consider a partial function $\Upsilon(m, X)$ for the

chain, within which the supersegment that has number m from the first end of the chain (and, consequently, number $\mathrm{N}-m$ from the second end of the chain) is localized at position X. The partial function of such a chain is equivalent to the product of partial functions for two chains, one containing m supersegments, and the other containing $\mathrm{N}-m$ supersegments, which both start from the origin and end at the same node within the shell number X. Since the shell number X contains κb^{X-1} nodes, to obtain partial function for the chain that ends at some specific node within the shell number X, the partial function (Z) for the chain that ends at the shell number X must be divided by κb^{X-1}. Thus, taking into account, that the chains could meet at any of κb^{X-1} nodes within the shell X, we obtain:

$$\Upsilon(m,X) \sim \frac{Z(m,X)}{\kappa b^{X-1}} \frac{Z(\mathrm{N}-m,X)}{\kappa b^{X-1}} \kappa b^{X-1} \sim a^{\mathrm{N}} \left(\frac{A^2}{b}\right)^X \frac{b}{\kappa}; \quad X \geq 1 \tag{42}$$

$$\Upsilon(m,0) = Z(m,0) Z(\mathrm{N}-m,0) = a^{\mathrm{N}} B^2 \tag{43}$$

(Here we substituted Eqs 37, 38 for the partial functions, assuming that m and $N-m$ are large enough to make these equations applicable) The probability for the supersegment number m (from the first end) to be within the shell X is

$$W(X) = \Upsilon(m,X) / \sum_{i=0}^{i=\infty} \Upsilon(m,i) = \left(\frac{A^2}{b}\right)^X \Bigg/ \left(\sum_{i=1}^{i=\infty} \left(\frac{A^2}{b}\right)^i + \frac{\kappa}{b} B^2 \right) \tag{44}$$

To render this probability non-zero, the sum $\sum_{i=1}^{i=\infty}\left(\frac{A^2}{b}\right)^i$ must converge, which occurs if

$$A < \sqrt{b} \tag{45}$$

If above condition is not fulfilled, then for any finite X probability Eq.44 is zero, which means that for infinitely long chain practically all internal segments move infinitely far from the origin. Consequently, for A exceeding the critical value

$$A_{cr} = \sqrt{b} \tag{46}$$

the fraction of adsorbed supersegments within infinitely long chain is zero.

From the Eq.46 we can obtain critical value for parameter υ (which is directly related to the free energy of winding (Eq.27)). For that, from Eqs.39, 40 we obtain

$$B = \frac{b}{\kappa} \tag{47}$$

which upon substituting into Eq.41 produces

$$a = \upsilon\left(\frac{\kappa}{b}A + 1\right) \tag{48}$$

Combining Eqs.48 and 39, we obtain interdependence between υ and A:

$$\upsilon = \frac{A^2 + A + b}{A^2 + (b/\kappa)A} \quad \frac{b}{\kappa} \tag{49}$$

which, upon substituting the critical value of A (Eq.46) produces

$$\upsilon_{cr} = \frac{2b + \sqrt{b}}{\kappa + \sqrt{b}} = \frac{2b + \sqrt{b}}{b + 1 + \sqrt{b}} \tag{50}$$

Eq.50 is a monotonically increasing function of b, which produces $\upsilon_{cr} = 1$ for $b = 1$, and approaching maximal value $\upsilon_{cr} \to 2$ when $b \to \infty$. Thus, for $b > 1$ (which is the case for our system), $\upsilon_{cr} > 1$, i.e., from Eq.27, υ_{cr} corresponds to some non-zero value of the free energy ΔG_λ. Consequently, there is some non-zero value of torque, below which there is no "adsorption", i.e., in the context of our model, the winding per segment is zero. Thus, the dependence of winding upon torque behaves as a phase transition. To define the character of the phase transition, we have to analyze the dependence of the fraction of adsorbed supersegments upon parameter υ (since υ (Eq.27) is a continuous strictly increasing function of the energy ΔG_λ, and ΔG_λ is a continuous strictly increasing function of torque, all conclusions about the character of the torque-dependent phase transition behavior could be made using υ as a variable instead of torque).

For this purpose, we note that from the Eq.30 it is seen, that when the walker either arrives at or stays in the origin (i.e. it becomes or remains adsorbed) the partial function is multiplied by υ. Thus, the partial function of those trajectories that have exactly m adsorbed supersegments would be υ^m times the term independent upon υ. From that, the average fraction of supersegments in the adsorbed state for the chain that ends in the origin is

$$\theta = \frac{1}{\mathrm{N}}\left(\frac{\partial \ln Z(\mathrm{N},0)}{\partial \ln \upsilon}\right)_{\kappa,b} = \frac{1}{\mathrm{N}}\left(\frac{\partial \ln Ba^{\mathrm{N}}}{\partial \ln \upsilon}\right)_{\kappa,b} = \left(\frac{\partial \ln a}{\partial \ln \upsilon}\right)_{\kappa,b} \tag{51}$$

In this notation, υ, κ and b are treated as independent variables.

(The right-most part of the equation (which does not depend upon the chain length and the end conditions, and generally corresponds to very long chains) in this case is exact, because parameter B doesn't depend upon υ (Eq.47)).

To determine function $a(\upsilon)$ (that is to be substituted in Eq.51) we first re-write Eq.49 as quadratic equation relative to A:

$$\left(\upsilon\frac{\kappa}{b} - 1\right)A^2 + (\upsilon - 1)A - b = 0 \tag{52}$$

which, since $\upsilon \geq 1$, has only one positive solution

$$A=\frac{-(\upsilon-1)+\sqrt{(\upsilon-1)^2+4(\upsilon\kappa-b)}}{2(\upsilon\kappa-b)}\,b=\frac{2b}{(\upsilon-1)+\sqrt{(\upsilon-1)^2+4(\upsilon\kappa-b)}} \tag{53}$$

Substituting Eq.53 into Eq.48, we obtain

$$a=\frac{2\kappa+\upsilon-1+\sqrt{(\upsilon-1)^2+4(\upsilon\kappa-b)}}{\upsilon-1+\sqrt{(\upsilon-1)^2+4(\upsilon\kappa-b)}}\,\upsilon \tag{54}$$

Substituting Eq.54 into Eq.51, we finally obtain the fraction of adsorbed supersegments as function of υ:

$$\theta=1-\frac{2\kappa\upsilon}{\left(\upsilon-1+\sqrt{(\upsilon-1)^2+4(\upsilon\kappa-b)}\right)\sqrt{(\upsilon-1)^2+4(\upsilon\kappa-b)}} \tag{55}$$

In the Appendix A we show that the above equation is strictly increasing function of υ (and consequently, of torque), and it crosses zero at some value of $\upsilon_{\theta=0}$:

$$\upsilon_{\theta=0}=\frac{2b+\sqrt{b}}{\kappa+\sqrt{b}} \tag{56}$$

This result coincides with Eq.50, i.e.

$$\upsilon_{\theta=0}=\upsilon_{cr} \tag{57}$$

That means that at critical point $\upsilon = \upsilon_{cr}$ (below which adsorption doesn't occur) the fraction of adsorbed supersegments is zero, and this fraction grows strictly and continuously with the growing of υ, when υ increases beyond the critical point. Thus, upon increase in torque, the system exhibits a second-order phase transition, where the fraction of adsorbed supersegments depends continuously upon torque, while its derivative experiences discontinuity at the critical value of torque.

(It is worth mentioning that the second-order character of the phase transition in our model (which involves random walk with a bias directed away from the "adsorbing surface") appears because, in the context of our system, we must take into account only those random walk trajectories that have both ends localized at the origin. If trajectories with one unconstrained end-point position were taken into account, then for a random walk biased away from the adsorbing surface (e.g. when an external force is applied to the free end of the chain) a first-order phase transition would emerge (reviewed in [9])).

The critical value of torque corresponds to the critical value of the parameter υ, which is directly related to the free energy of winding (Eq.27). Although there is no exact analytical expression for the dependence between the free energy of winding (and, consequently, parameter υ) and the torque, an appropriate approximation could be chosen from the following consideration:

Because $\upsilon_{cr} < 2$ (see Eq.50 and comments below), the free energy of the adsorbed supersegment at the critical point

$$\left(-\Delta G_{\lambda}\right)_{cr} = kT \ln \upsilon_{cr} < kT \ln 2 < kT \tag{58}$$

(For example, for 2D-grid $\beta = 3,\ \upsilon_{cr} \approx 1.35$, and $\left(-\Delta G_{\lambda}\right)_{cr} \approx 0.3kT$.)

This means that in the critical point, the shape of adsorbed supersegment is relatively weakly perturbed by torque; consequently, at the critical point Eq.20 for small deformations is applicable.

Thus

$$\left(-\Delta G_{\lambda}\right)_{cr} \approx \frac{kT}{2}\left(q_{cr}\phi_{\lambda T}\right)^2 \tag{59}$$

and from that and Eqs.22, 27, 50

$$q_{cr} = \frac{\sqrt{2\left(-\Delta G_{\lambda}\right)_{cr}/kT}}{\phi_{\lambda T}} = \frac{\sqrt{2\ln\upsilon_{cr}}}{\phi_{\lambda T}} \sim \frac{\sqrt{\ln\left(\left(2b+\sqrt{b}\right)/\left(b+1+\sqrt{b}\right)\right)}}{\ln\left(\lambda/l\right)^2} \tag{60}$$

Thus, the critical torque decreases with increase in the size of the cage λ.

We can obtain the general winding-torque interdependence $u(q)$ (where $u \equiv \langle\phi\rangle/N$ is the average winding per segment, $q \equiv M/kT$ is the normalized torque), taking into account that the average winding per segment is equivalent to the winding per segment in the adsorbed state (u_{λ}) times the fraction of adsorbed supersegments:

$$u = u_{\lambda}(q)\,\theta\big(\upsilon(q)\big) \tag{61}$$

At sufficiently small torques, when the size of the torsional blob (Eq.14) is larger then the size of the cage, $u_{\lambda}(q)$ can be evaluated using Eqs.18, 21, 22:

$$u_{\lambda}(q) \equiv \frac{\langle \phi_{\lambda} \rangle}{n_{\lambda}} \sim \frac{q\phi_{\lambda T}^{2}}{n_{\lambda}} \sim \frac{q\ \big(\ln(\lambda/l)\big)^{2}}{(\lambda/l)^{2}} \tag{62}$$

In the opposite situation, the regions of the chain within the central cage wouldn't "feel" the cage, and $u_{\lambda}(q)$ could be evaluated from Eq.13.

The function $\theta(\upsilon)$ is given by Eq.55, which is valid for all torques that exceed the critical value, below which $\theta = 0$. The function $\upsilon(q)$ could be evaluated from Eq.27, where the free energy of a supersegment within the central cage, $\Delta G_{\lambda}(q)$, is given either by Eqs.20, 23, or Eq.15 (with replacement n_{λ} for N), depending upon whether the size of the torsional blob is larger or smaller the size of the cage, respectively. Note that the functions $\upsilon(q)$ and $u_{\lambda}(q)$ do not have any discontinuities, and consequently the character of the phase transition in the winding-torque interdependence is completely defined by the function $\theta(\upsilon)$.

Another important parameter, which can be evaluated from the partial function of the chain is an average size for a loop between two continuous stretches of the chain in the adsorbed state.

For that, note that each time the chain is leaving an adsorbed state (i.e. starts a loop) the partial function is multiplied by κ. From that, using the same reasoning, as for Eq.51, the number of loops normalized upon the total number of supersegments (further referred as the junction density) is:

$$J = \frac{1}{\mathrm{N}}\left(\frac{\partial \ln Z(\mathrm{N},0)}{\partial \ln \kappa}\right)_{\upsilon,b} = \frac{1}{\mathrm{N}}\left(\frac{\partial \ln Ba^{\mathrm{N}}}{\partial \ln \kappa}\right)_{\upsilon,b} \approx \left(\frac{\partial \ln a}{\partial \ln \kappa}\right)_{\upsilon,b} \tag{63}$$

(The right-most part of the equation corresponds to approximation for very long chains, and, since we are interested in very long chains, below it will be used as exact equality.) The average number of supersegmens within one loop, and within one uninterrupted stretch of adsorbed supersegments between the loops is $(1-\theta)/J$ and θ/J, respectively. The exact expression for these values are given in Appendix B; here we only mention that at the critical point, the characteristic length of a "seed" of adsorbed phase is finite, while loops (for the infinitely long chain) are infinitely long. Note that the very long loops in the vicinity of the phase transition support self-consistency of our simplified model, in which we neglect the winding of the regions outside the central cage: because the maximal possible winding of these regions is limited (see the beginning of the current subsection), and this limitation does not depend upon the length of the region, the longer the region, the smaller maximal possible winding per segment within the region, and, consequently the better is the approximation that the winding per segment within the region is zero.

C. Effect of non-topological obstacles upon torque-winding interdependence.

We model non-topological obstacles as impenetrable spherical objects with the characteristic size larger than the chain segment, but small in comparison with the scale describing the chain distribution in space (e.g. the average distance from the cylinder.). We also assume that the percentage of volume occupied by the obstacles is small.

The effect of non-topological obstacles is convenient to analyze using an analogy between the Gaussian polymer chain and the path of a diffusing particle:

The probability W for the end of the chain to be a certain point r is the same as the respective probability for a diffusing particle, provided that the time (t) passed since the particle left the origin is replaced by the number of segments within the chain N, and the diffusion coefficient (D) of the particle is replaced by $l^2/2$. (The value l^2 is the squared length of the segment divided by dimensionality of the system. For example, for a 3D-chain the length of the segment is $l\sqrt{3}$. For estimations up to numerical constants, l could be simply referred to as the length of the segment.)

In the continuous approximation, the probability for the end of the chain to be at the surface of an impenetrable obstacle is zero. In terms of particle analogy, such a boundary condition means the irreversible disappearance of the particle upon collision with the obstacle. Taking into account that the probability to find a particle at some position in space is proportional to the particle concentration C in this position, we can describe interaction of the particle with the obstacle in terms of irreversible "chemical" reaction between the particle and the obstacle, which leads to the kinetic equation:

$$\frac{\partial C}{\partial t} = D\nabla^2 C - k_f c_{obst} C \tag{64}$$

where c_{obst} is concentration of obstacles, and k_f is the forward rate constant for the "reaction" between the particle and the obstacles, which is related to the characteristic size of the obstacle ς by Smoluchowski equation:

$$k_f = 2\pi D\,\varsigma \tag{65}$$

(Numerical coefficient in the above equation corresponds to spherical particles with diameter equivalent to the characteristic size of the obstacles.)

Based upon described above analogy between the polymer chain and diffusing particle, by substituting into Eq.64 the probability for the end of the chain location W for the particle concentration C, the number of segments N for the time t, and $l^2/2$ for D, we obtain

$$\frac{\partial W}{\partial N} = \frac{l^2}{2}\left(\nabla^2 W - 2\pi\varsigma c_{obst} W\right) \tag{66}$$

(An alternative derivation of this equation without particle analogy is given in Appendix C)

Applying to Eq.66 the same procedures like for Eq.1 (i.e. Eqs 2, 3), we obtain equation for the partial function of the chain in the presence of torque

$$\frac{\partial W_M}{\partial N} = \frac{l^2}{2}\left(\frac{\partial^2 W_M}{\partial r^2} + \frac{1}{r}\frac{\partial W_M}{\partial r} + \left(\frac{\left(\frac{M}{kT}\right)^2}{r^2} - 2\pi\varsigma c_{obst} \right) W_M \right) \tag{67}$$

With the exception of the term containing concentration of obstacles, the above equation is the same as Eq.4.

In this Schrodinger-type equation, the term in front of the partial function could be interpreted as a potential energy (taken with minus sign and divided by kT) of a segment of the chain localized at the point r (reviewed in [11]).

Thus, in this case an apparent potential energy is

$$U = kT\, l^2 \left(-\left(M/kT\right)^2 / r^2 + 2\pi\varsigma c_{obst} \right) / 2 \tag{68}$$

The torque-containing term creates an apparent attractive inverse squared potential [4]. The obstacles create an additional repulsive potential, which is proportional to their concentration c_{obs}. If the concentration grows with the distance from the cylinder, that would create apparent attractive force, causing the chain to move closer to the cylinder. That would decrease the chain resistance against winding, and consequently, produce greater winding at a given torque. In the opposite situation, in which the concentration of obstacles decreases with the distance from the cylinder, they would create an apparent

repulsive force moving the chain away from the cylinder. That would increase resistance of the chain against winding, and, consequently, produce smaller winding for a given torque. (If the concentration of non-topological obstacles doesn't change with the distance from the cylinder, then they do not affect torque-winding interdependence.)

Here we are not analyzing the detailed features of torque-winding interdependence for a general case $c_{obs}(r)$. However, we mention an interesting special case, in which the concentration decreases as an inversed squared distance from the axis of the cylinder (i.e. in the same way as the torque-dependent term):

$$c_{obst}(r) = \frac{\alpha}{r^2} \tag{69}$$

where α is some constant.

In this case, Eq.67 is equivalent to the equation for the chain under constant torque in the absence of obstacle (which analyzed in details in [3], and the obtained results are briefly summarized in the first subsection of the Results), provided that in the equation the actual torque M is replaced by an apparent torque:

$$M_{apparent} = \sqrt{M^2 - 2\pi\alpha(kT)^2\varsigma} \tag{70}$$

Upon decrease in actual torque M, an apparent torque (Eq.70) and, consequently, directed (non-random) winding, would decrease until they both reach zero at the critical value of torque

$$M_{cr} = kT\sqrt{2\pi\varsigma\alpha} \tag{71}$$

From the physical considerations, upon decrease of the torque below the critical value (Eq.71) the directed winding should remain zero: really, it can not become positive again because this would mean that directed winding increases upon decrease in torque, which doesn't make physical sense; and it cannot become negative, because, since the obstacles distributed symmetrically, they cannot produce actual torque acting in the opposite direction. Thus, for the profile of concentration of obstacles described by Eq.69, the dependence of the winding upon the torque exhibits a phase transition. To characterize this transition, we substitute the asymptotic equation for small torques (Eq.16) (with $q_{apparent} \equiv M_{apparent}/kT$ instead of $q \equiv M/kT$) into the Eq.15 for the free energy of winding:

$$\Delta G \approx -NkT\frac{l^2}{2R^2}\exp\left(-2\pi/q_{apparent}\right) \tag{72}$$

It is seen that, due to the presence of the term exponential upon $q_{apparent}^{-1}$, all derivatives of the free energy (Eq.72) are approaching zero when $q_{apparent}$ approaches zero (which

corresponds to the transition point). Thus, in the transition point, all derivatives are continuous, i.e. this phase transition could be viewed as an "infinitely smooth".
Here we want to emphasize that, according to our analysis, the phase transition within torque-winding interdependence in our system occurs only in the presence of obstacles; in the absence of obstacles, there is a finite non-zero winding for any finite non-zero value of torque (Eq.13). That is in contrast to conclusion made in [4] about the presence of an infinitely smooth phase-transition for a similar (but not identical) system that comprises only the cylinder (rod) and the polymer chain, but with no additional obstacles. Understanding the origin of this difference with our results would require further investigations.

We have considered fixed concentration profiles of the non-topological obstacles.
Now we will briefly consider what happens if the chain wound around a cylinder is placed in initially homogeneous solution of non-topological obstacles, and these obstacles are allowed to re-distribute in space. Because an obstacle and a segment of the chain cannot be localized in the same place in space, the presence of the chain segments reduces the space available for the obstacles. That would create entropical forces acting upon the obstacles in the direction towards decrease in the concentration of the chain segments, which is (except in a very close vicinity of the cylinder) pointed away from the cylinder. As a result, the concentration of obstacles would increase with the distance from the cylinder, which, as we discuss above, would push the chain toward the cylinder thus decreasing the chain's resistance to the torque.

III. DISCUSSION

In this work, we have studied the effect of topological and non-topological obstacles (Fig.1) upon torque-winding interdependence for a flexible polymer chain wound around an impenetrable cylinder.

In the presence of topological obstacles not linked with the chain (Fig.1B), the region of the chain protruded between these obstacles has dramatically decreased capacity to respond to torque by winding around a cylinder (Fig.2). Based upon that, we model a chain embedded in an array of such an obstacles, as comprised of elements in two possible states: ones that are localized within the same cage as the cylinder and are responsive to torque, and ones localized within loops extruded from this cage, which are not able to wind around the cylinder, and, consequently, are not responsive to torque (Fig.3A). Within this approximation, the torque-winding interdependence has a character of second-type phase transition (formally similar to one that occurs upon polymer adsorption on the surface): below some critical value of torque, the directed winding is zero; and when torque exceeds this critical value, the winding starts to grow continuously (from zero value) upon increase in torque. It remains to be tested how the assumptions made within this approximate model affect the phase-transition-like behavior.

Another interesting question is how introducing a disorder in the array of topological obstacles (including irregularities in their spatial distribution, orientation, and shape) would affect the chain behavior. In general, regular arrays of topological obstacles are often used to model irregular systems like gels or polymer melts (reviewed in [11]);

however, a question of how irregularities affect critical behavior of the system is certainly not trivial. In the framework of our simplified description of the system, random irregularities within the array of topological obstacles could be modeled as fluctuations in the parameters of the system, in particular, fluctuation of the apparent adsorption energy, which depends upon the "cage" size, and, consequently, would fluctuate with the fluctuation of the distance between the obstacles due to irregularities in the array. In this aspect, the effect of disorder in the array of obstacles would be reminiscent of the adsorption of a polymer chain on a random heterogeneous surface, which, like in the case of homogeneous surface, also exhibits critical desorption-adsorption transition, though in the case of heterogeneous surface, its analysis is more complicated (e.g. [18] and the references wherein).

Note that in any case, the presence of topological obstacles renders the winding-torque interdependence to be more "phase-transition-like" because of the "contrasting" effect upon the difference in torsional compliances between the cylinder-proximal and the cylinder-distal regions of the chain.

In this work, we have analyzed only an ideal polymer chain without excluded volume. The excluded volume effects for closed unlinked loops in the array of obstacles might be very significant for long loops (e.g. see [19]), though in our case they could be partially alleviated by the possibility for the chain to shift along the axis of the cylinder. However, the basic mechanism for the phase-transition-like behavior, the rendering the protruded loops irresponsive to torque, would remain the same for real polymers; thus, in this case

phase-transition-like behavior also could be expected. Also, similar effect of topological obstacles could be expected for two flexible polymer chains wound around each other.

In contrast to topological obstacles, non-topological obstacles (Fig.1C) affect torque-winding only if concentration of obstacle changes with the distance from the cylinder: if this concentration increases with the distance from the cylinder, that would facilitate the chain getting closer to the cylinder, making the chain's resistance against winding smaller; if the concentration decreases with the distance from the cylinder, the effect would be opposite. At least at some profiles of the non-topological obstacles concentrations, the winding-torque interdependence also has character of the phase transition.

An interesting situation appears when the chain wound around the cylinder is placed into initially homogeneous solution of freely moving non-topological obstacles: In this case the chain displaces the obstacles away from the cylinder, which in turn "pushing" the chain towards the cylinder and making it more prone to winding and, consequently, more compliant to torque. The decrease of the distance between the chain and the cylinder due to the presence of the non-topological obstacles raises an interesting question how these obstacles affect viscous resistance for the polymer chain rotation around the cylinder: on one hand, the presence of impenetrable particles (i.e. non-topological obstacles) increases an apparent viscosity of the solution, thus increasing resistance; on the other hand, decreasing the distance between the chain and the cylinder decreases linear velocity of the chain's segments (at a given angular velocity), and the lever arm for frictional forces, thus decreasing resistance. Quantitative analysis of this effect remains to be done.

In terms of potential biological implications, as described in detail in [3, 8], the model of flexible chain wound around a cylinder could be relevant for transcription, in the case in which the RNA transcript becomes anchored to DNA. Since transcription usually occurs in the crowded environment created by other macromolecules, the effect of obstacles in this case is likely to be important.

Another biological system including intertwined polymers, in which the effects of obstacles (especially topological) could be important, are intertwined nascent DNA duplexes within the replication bulge called "pre-catenanes" [20]. Within the cells, chromosomes are usually very "crumpled", and the characteristic times for their rearrangements in space are very slow (reviewed in [21]). Thus, if pre-catenanes are formed in some region within a chromosome, then neighboring (in terms of location in space) regions of this or other chromosomes could play a role as topological obstacles.

Previously [3, 7], the results obtained for a static polymer chain wound around the cylinder (in particular, the relationship between the torque and the characteristic size) were extrapolated to the dynamic situation in which the chain is rotating around the cylinder with only one end attached to its surface (The latter system could model rotation of the nascent RNA around DNA during transcription, which could generate transient superhelical stress [22, 23]). This extrapolation is similar to the "trumpet" model, in which the relationship between the stretching force and the characteristic size obtained for the static force [12] was extrapolated to a moving polymer pulled by the force in viscous environment [24, 25]. In the case of non-topological obstacles this extrapolation, in principle, could be done similarly as in the absence of obstacles [3], though mathematically the dependence between the characteristic size and the torque would be

more complicated. In the case of topological obstacles, the possibility of such extrapolation is not obvious, because the free end might thread in between the obstacles. In general, the effect of obstacles upon the rotation of the polymer chain in the viscous environment (as well as upon related process of spontaneous polymer unwinding (e.g. [26])) is worth exploring.

In conclusion, because various processes involving static or dynamic strains within polymers (e.g. transcription) often occur in a crowded environment (e.g. in living cells), including in the model the effect of obstacles is of significant interest.

ACKOWLEDGMENTS

I thank Prof. P. C. Hanawalt, in whose laboratory this work was performed, for support, critical reading of the manuscript and helpful suggestions. The work was supported by a grant, CA077712, from the National Cancer Institute, NIH, to Hanawalt's laboratory at Stanford University.

APPENDIX A: ANALYSIS OF THE DEPENDENCE $\theta(v)$.

Though the parameter υ is directly linked with the winding energy (Eq.27), and, consequently, the torque, it is more convenient to express all functions of interest via parameter A.

First, let us prove that υ is strictly decreasing function of A:

By differentiation of the Eq.49 we obtain

$$\left(\frac{\partial \upsilon}{\partial A}\right)_{\kappa,b} = -\frac{(b/\kappa)\left(b-A^2\right)+A^2+2bA}{\left(A^2+(b/\kappa)A\right)^2}\ \frac{b}{\kappa} \qquad \text{A1}$$

It is seen that for $0 \le A \le A_{cr} = \sqrt{b}$ (i.e. within the whole area of interest) the above expression is strictly negative, thus the function $\upsilon(A)$ is strictly decreasing.

Next, from Eq.39 we obtain:

$$a = \frac{A^2+A+b}{A} \qquad \text{A2}$$

Because the above equation doesn't contain either υ or κ, we can present Eq.51 in the form

$$\theta = \left(\frac{\partial \ln a}{\partial \ln \upsilon}\right)_{\kappa,b} = \left(\frac{\partial \ln a}{\partial A}\right)_{b} \left(\frac{\partial A}{\partial \ln \upsilon}\right)_{\kappa,b} \qquad \text{A3}$$

where the derivative $\left(\partial \ln a/\partial A\right)_b$ can be obtained by taking the logarithm of Eq.A2 and differentiating by A:

$$\left(\frac{\partial \ln a}{\partial A}\right)_b = \left(\frac{\left(\ln\left(A^2+A+b\right)-\ln A\right)}{\partial A}\right)_\beta = \frac{2A+1}{A^2+A+b} - \frac{1}{A} = -\frac{b-A^2}{A\left(A^2+A+b\right)} \qquad \text{A4}$$

To obtain $\left(\partial A/\partial \ln \upsilon\right)_{\kappa,b}$ it is convenient to take logarithm of Eq.49:

$$\ln \upsilon = \ln b - \ln \kappa + \ln\left(A^2+A+b\right) - \ln A - \ln\left(\frac{b}{\kappa}+A\right) \qquad \text{A5}$$

and differentiate both sides of the Eq.A5 by $\ln \upsilon$ at constant κ and b:

$$1 = \left(\frac{2A+1}{A^2+A+b} - \frac{1}{A} - \frac{1}{\frac{b}{\kappa}+A}\right)\left(\frac{\partial A}{\partial \ln \upsilon}\right)_{\kappa,b} \qquad \text{A6}$$

or

$$\left(\frac{\partial A}{\partial \ln \upsilon}\right)_{\kappa,b} = -\frac{A\left(A^2+A+b\right)\left(\frac{b}{\kappa}+A\right)}{A^2\left(1-\frac{b}{\kappa}\right)+2bA+\frac{b^2}{\kappa}} \qquad \text{A7}$$

Substituting Eqs.A4,A7 into Eq.A3, we obtain:

$$\theta = \frac{\left(b - A^2\right)\left(A + \frac{b}{\kappa}\right)}{A^2\left(1 - \frac{b}{\kappa}\right) + 2bA + \frac{b^2}{\kappa}} \qquad \text{A8}$$

It is seen, that the above equation turns zero at

$$A_{\theta=0} = \sqrt{b} \qquad \text{A9}$$

Thus, from Eqs.46 and A9, $A_{\theta=0} = A_{cr}$, and, consequently, $\upsilon_{\theta=0} = \upsilon_{cr}$.

To prove that the function $\theta(A)$ (Eq.A8) is strictly decreasing, it is convenient to introduce auxiliary function

$$\Theta = \frac{1}{\frac{1}{\theta} - 1} = \frac{\theta}{1 - \theta} \qquad \text{A10}$$

and note that if $\theta(A)$ is strictly decreasing, then $\Theta(A)$ is also strictly decreasing, and vice versa.

Substituting Eq.A8 into Eq.A10 we obtain

$$\Theta(A)=\left(b-A^2\right)\left(1+\frac{b}{\kappa}\frac{1}{A}\right)\left(\frac{1}{A^2+A+b}\right) \qquad \text{A11}$$

In the area of interest (i.e. $0 \le A \le A_{cr} = \sqrt{b}$), Eq.A11 is a product of three strictly decreasing functions, two of which are strictly positive, and one is not negative. It can be seen from straight-forward differentiation, that the derivative of such a product is strictly negative. Thus, $\Theta(A)$, and, consequently, $\theta(A)$ are strictly decreasing functions; and, since $\upsilon(A)$ is strictly decreasing function, we finally conclude that the function of interest, $\theta(\upsilon)$, is strictly increasing function.

APPENDIX B: DERIVATION OF EXPRESSION FOR THE JUNCTION DENSITY AND FOR THE CHARACTERISTIC SIZES OF CONTINUOUS STRETCHES OF ADSORBED AND NON-ADSORBED SEGMENTS.

To calculate the junction density we will use the same approach as in the previous Appendix, except interchanging υ for κ.

Similar to Eq.A3, we present Eq.63 for the junction density in the form

$$J = \left(\frac{\partial \ln a}{\partial \ln \kappa}\right)_{\upsilon,b} = \left(\frac{\partial \ln a}{\partial A}\right)_{b} \left(\frac{\partial A}{\partial \ln \kappa}\right)_{\upsilon,b} \qquad \text{B1}$$

By differentiation of Eq.A5 by $\ln\kappa$ at constant υ and b we obtain:

$$\left(\frac{\partial A}{\partial \ln \kappa}\right)_{\upsilon,b} = -\frac{\left(A^2 + A + b\right)\left(A + \frac{b}{\kappa}\right)A}{A^2\left(1 - \frac{b}{\kappa}\right) + 2bA + \frac{b^2}{\kappa}} \quad \frac{A}{A + \frac{b}{\kappa}} \qquad \text{B2}$$

Substituting Eqs.A4, B2 into Eq.B1 , we obtain the junction density

$$J = \frac{\left(b - A^2\right)A}{A^2\left(1 - \frac{b}{\kappa}\right) + 2bA + \frac{b^2}{\kappa}} \qquad \text{B3}$$

From Eqs.A8 and B3, the average number of adsorbed supersegments in one uninterrupted stretch

$$\xi_{adsorbed} = \frac{\theta}{J} = \frac{A + \frac{b}{\kappa}}{A} = 1 + \frac{b}{A\kappa} \qquad \text{B4}$$

and the average number of non-adsorbed supersegments in one uninterrupted stretch (i.e. in the loop)

$$\xi_{loop} = \frac{1-\theta}{J} = \frac{A^2 + A + b}{b - A^2} \qquad \text{B5}$$

It is interesting to note that at the critical point $A_{cr} = \sqrt{b}$ the uninterrupted stretches of adsorbed supersegments (Eq.B4) have finite size

$$\xi_{adsorbed(cr)} = 1 + \frac{b}{\kappa\sqrt{b}} = 1 + \frac{\sqrt{b}}{(b+1)} \qquad \text{B6}$$

while the loops (Eq.B5) are infinitely long.

APPENDIX C: ALTERNATIVE DERIVATION OF DIFFUSION-TYPE EQUATION FOR THE PARTIAL FUNCTION IN THE PRESENCE OF THE NON-TOPOLOGICAL OBSTACLES.

Consider Gaussian polymer chain containing N segments (characteristic length of one segment is $l\sqrt{3}$), in the Cartesian coordinates (x,y,z).

Let consider a discretized model, in which the space is represented as a grid comprised of cubic cells with the lengths of the sides equivalent to the characteristic size of the obstacle ς. (This approach to the space representation was used before in [27] in the context of proteins searching for their targets). Then, new coordinates in the frame of the grid (in which the distance between neighboring cells is equivalent to unity) are:

$$x_\varsigma = x/\varsigma; \quad y_\varsigma = y/\varsigma; \quad z_\varsigma = z/\varsigma \qquad \text{C1}$$

The chain can be represented as comprising of "supersegments" with the characteristic size equivalent to the size of the obstacle. Each of this supersegments contains $\left(\varsigma/l\sqrt{3}\right)^2$ segments, thus the number of supersegments in the chain

$$N_\varsigma = \frac{N}{\left(\varsigma/l\sqrt{3}\right)^2} \qquad \text{C2}$$

For the end of the chain containing N_ς supersegments to occur at certain position, it is required that (i) this position is not occupied by an obstacle, and (ii) the preceding segment is localized in one of six neighboring positions.

Thus, the recurrence equation for the probability $W\left(N_\varsigma, x_\varsigma, y_\varsigma, z_\varsigma\right)$ for the end of the chain to be in a certain position is

$$W\left(N_\varsigma,x_\varsigma,y_\varsigma,z_\varsigma\right)=\frac{1}{6}\left[1-p\left(x_\varsigma,y_\varsigma,z_\varsigma\right)\right]\left[W\left(N_\varsigma-1,x_\varsigma\pm1,y_\varsigma,z_\varsigma\right)+W\left(N_\varsigma-1,x_\varsigma,y_\varsigma\pm1,z_\varsigma\right)+W\left(N_\varsigma-1,x_\varsigma,y_\varsigma,z_\varsigma\pm1\right)\right] \quad \text{C3}$$

Here $p\left(x_\varsigma,y_\varsigma,z_\varsigma\right)$ is the probability that respective position is occupied by an obstacle, and the factor 1/6 appears, because, since in 3D –space each cubic cell has six immediate neighbors, thus the probability to "step" into a specific neighboring cell is 1/6. Notation "$\pm$" in this context means the sum of terms W with plus and with minus (e.g. $W\left(N_\varsigma-1,x_\varsigma\pm1,y_\varsigma,z_\varsigma\right)\equiv W\left(N_\varsigma-1,x_\varsigma+1,y_\varsigma,z_\varsigma\right)+W\left(N_\varsigma-1,x_\varsigma-1,y_\varsigma,z_\varsigma\right)$).

Assuming that p is sufficiently small, so that $1/(1-p)$ could be replaced by $1+p$, and expanding W into Taylor series for N_ς and for coordinates (and keeping only lowest order non-zero terms), we obtain continuous version of Eq.C3:

$$\frac{\partial W}{\partial N_\varsigma}=\frac{1}{6}\left(\frac{\partial^2 W}{\partial x_\varsigma^2}+\frac{\partial^2 W}{\partial y_\varsigma^2}+\frac{\partial^2 W}{\partial z_\varsigma^2}\right)-pW \quad \text{C4}$$

Substituting Eqs.C1, C2 into Eq.C4, and taking into account that for small concentrations of obstacles

$$p\approx\varsigma^3 c_{obst} \quad \text{C5}$$

we obtain

$$\frac{\partial W}{\partial N} = \frac{l^2}{2}\left(\nabla^2 W - 6\,\varsigma c_{obst} W\right) \qquad \text{C6}$$

That coincides with Eq.66 (up two numerical coefficient at concentration term, which depends upon the shape of an obstacle, and consequently, is not expected to be reproduced in this derivation).

References

[1] S. F. Edwards, Proceedings of the Physical Society of London **91**, 513 (1967).
[2] A. Grosberg and H. Frisch, Journal of Physics a-Mathematical and General **36**, 8955 (2003).
[3] B. P. Belotserkovskii, Phys Rev E Stat Nonlin Soft Matter Phys **89**, 022709 (2014).
[4] C. Nisoli and A. R. Bishop, Physical Review Letters **112**, 070401 (2014).
[5] F. Weysser, O. Benzerara, A. Johner and I. M. Kulic, Soft Matter **11**, 732 (2015).
[6] J. C. Walter, M. Laleman, M. Baiesi and E. Carlon, European Physical Journal-Special Topics **223**, 3201 (2014).
[7] M. Laleman, M. Baiesi, B. P. Belotserkovskii, T. Sakaue, J. C. Walter and E. Carlon, Macromolecules **49**, 405 (2016).
[8] B. P. Belotserkovskii and P. C. Hanawalt, Biophys J **100**, 675 (2011).
[9] L. I. Klushin and A. M. Skvortsov, Journal of Physics a-Mathematical and Theoretical **44** (2011).
[10] E. M. Ferreira and J. Sesma, Numerische Mathematik **16**, 278 (1970).
[11] A. Y. Grosberg and A. R. Khokhlov, *Statistical Physics of Macromolecules* (Springer-Verlag, New York, 1994).
[12] P. Pincus, Macromolecules **9**, 386 (1976).
[13] J.-C. Walter, G. Barkema and E. Carlon, J. Stat. Mech.: Theory Exp (2011).
[14] S. Nechaev, International Journal of Modern Physics B **4**, 1809 (1990).
[15] A. R. Khokhlov and S. K. Nechaev, Physics Letters A **112**, 156 (1985).
[16] S. K. Nechaev, A. N. Semenov and M. K. Koleva, Physica A **140**, 506 (1987).
[17] R. J. Rubin, Journal of Chemical Physics **43**, 2392 (1965).
[18] J. D. Ziebarth, Y. M. Wang, A. Polotsky and M. B. Luo, Macromolecules **40**, 3498 (2007).

[19] J. Smrek and A. Y. Grosberg, Journal of Physics-Condensed Matter **27**, 064117 (2015).
[20] A. I. Alexandrov, N. R. Cozzarelli, V. F. Holmes, A. B. Khodursky, B. J. Peter, L. Postow, V. Rybenkov and A. V. Vologodskii, Genetica **106**, 131 (1999).
[21] J. D. Halverson, J. Smrek, K. Kremer and A. Y. Grosberg, Reports on Progress in Physics **77**, 022601 (2014).
[22] L. F. Liu and J. C. Wang, Proc Natl Acad Sci U S A **84**, 7024 (1987).
[23] Y. P. Tsao, H. Y. Wu and L. F. Liu, Cell **56**, 111 (1989).
[24] F. Brochard-Wyart, Europhys. Lett. **23**, 105 (1993).
[25] F. Brochard-Wyart, Europhys. Lett. **30**, 387 (1995).
[26] J. C. Water, M. Baiesi, E. Carlon and H. Schiessel, Macromolecules **47**, 4840 (2014).
[27] S. E. Halford and J. F. Marko, Nucleic Acids Research **32**, 3040 (2004).

FIGURE LEGENDS

Fig.1. Flexible polymer chain wound around the cylinder.

Polymer chain is shown in black; the cylinder shown in gray. A: Obstacles are absent. At the right, a view along the axis of the cylinder (in which the cylinder appears as a small grey circle) is shown to demonstrate that in order to form the same winding angle (the angle between two dashed lanes emanating from the center of the cylinder), the region localized farther from the center of the cylinder must be stretched stronger than the region of the same length localized closer to the cylinder. B: Topological obstacle (shown as a thinner cylinder). When protruded around such an obstacles, the chain has to re-trace its way back, which is more clearly seen at the projection along the axis of the cylinders at the right. C: Non-topological obstacles, shown as gray circles.

Fig.2. The winding angle for the region extruded between topological obstacles. The figure is projection along the axis of the cylinder. The junctions of the extruded region are defined as crossing points between the chain and the line that is connecting the obstacles (which are numerated as **1**, **2**, **3**). It is seen that the winding angle of the extruded region (which is the angle between two solid arrowed lines; shown for obstacles **1** and **2**) cannot exceed the angle between dashed arrowed lines emanating from the center of the cylinder and ending at the obstacles. An important special case (the obstacles **2** and **3)** is when both obstacles and the center of the cylinder are lying on the same line. In this case, the winding of the cut out extruded region (at the right from the line) is exactly zero.

Fig.3. The chain wound around a cylinder embedded into an array of topological obstacles. A: The figure is projection along the axis of the cylinder. The chain is shown as a black line, the cylinder is shown as a larger gray circle, and obstacles are shown as smaller gray circles. The area in between four closest obstacle with borders shown by dashed lines is referred to as a "cage", and together the cages form a "grid". The cage containing the cylinder is referred as a "central cage". An example of a "ray" emanating from the center of the cylinder is shown as a dotted line. For the loop cut out by this ray, the winding angle is zero. B: Simplified representation of the picture in A, where actual coils of the chain are replaced by "supersegments" (see the text for detailed explanation). Outside the central cage, supersegments are shown by black arrowed lines. Inside the central cage supersegment are not shown, and the central cage is shown as a gray box, in

which supersegments are “adsorbed”. C: Cayley tree representation of the chain trajectory in B. To build a Cayley tree from a grid, the lines are emanated from the central cage to the middle of four neighboring cages (the ones that shares borders with the central cage) forming the first shell of nodes, then the lines are emanating from the cages of the first shell to the neighboring cages (except the central one) forming nodes of the second shell, and so on. The nodes of shells are connected by dotted lines, and the shell’s number is designated as X (for the central cage, $X = 0$)

Fig.4. Non-closed random walk trajectory on Cayley tree.

In this example, end-point is located at $X = 2$.

Fig.5. Non-zero coordinate on the Cayley tree might correspond to zero coordinate in real space.

The loop, which on the Cayley tree ends in the fourth shell (left) in real space is protruded into the central cage (right).

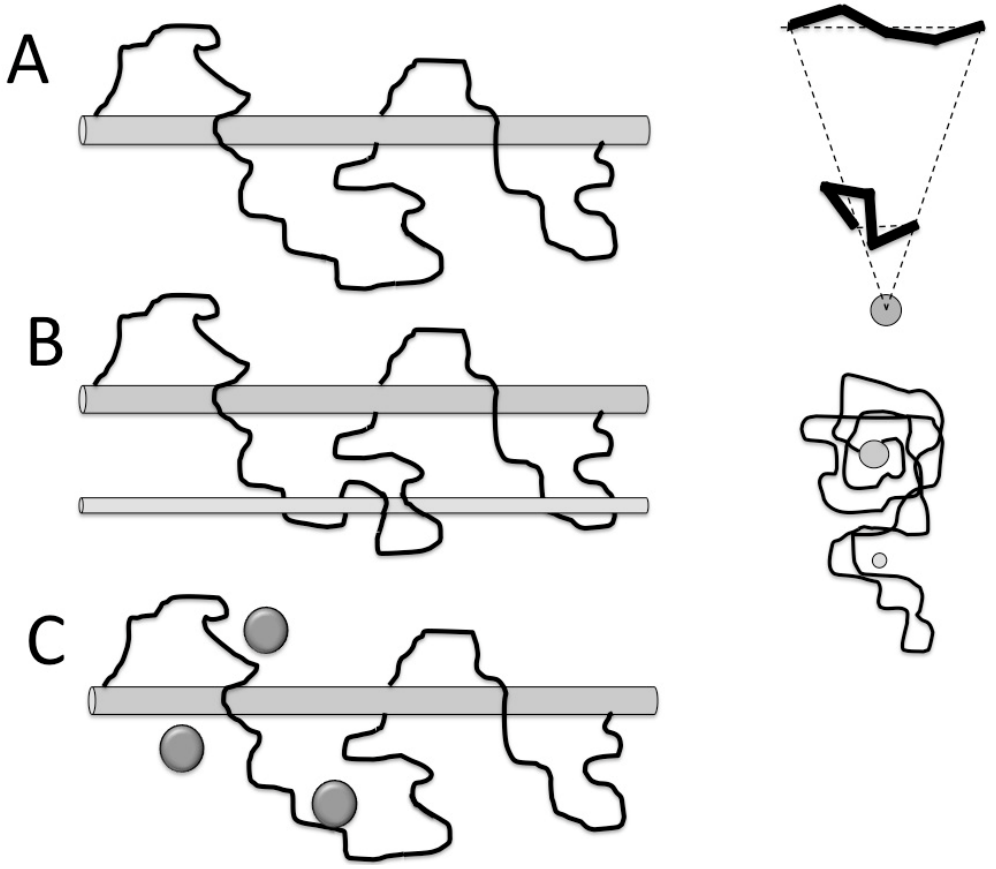

Fig.1

Fig.2

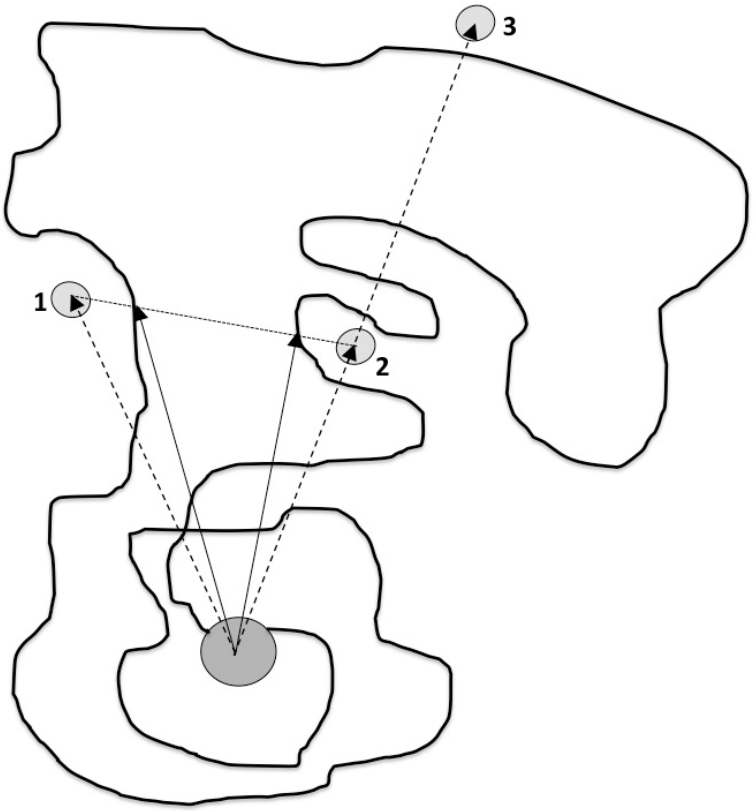

Fig.3

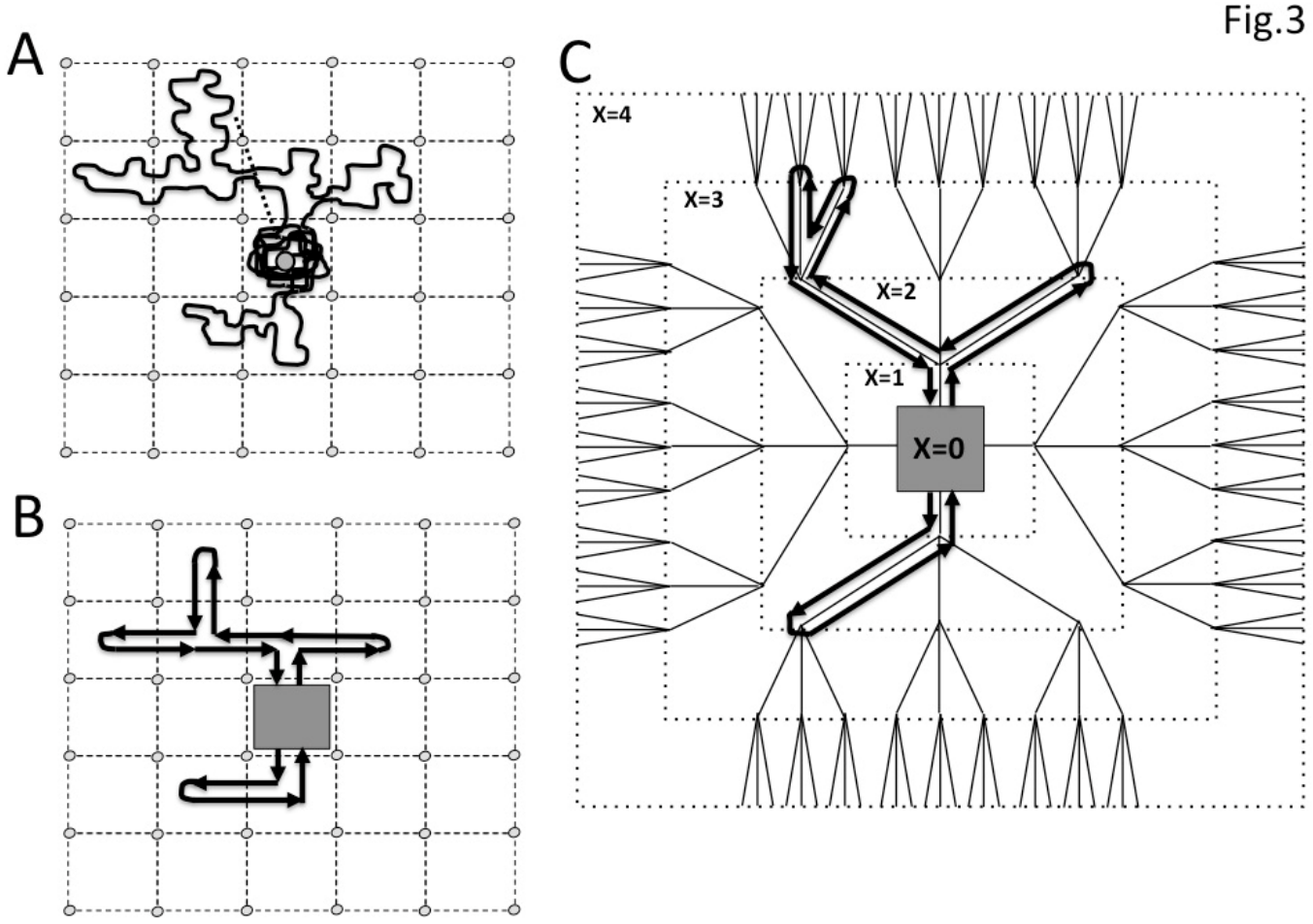

Fig.4

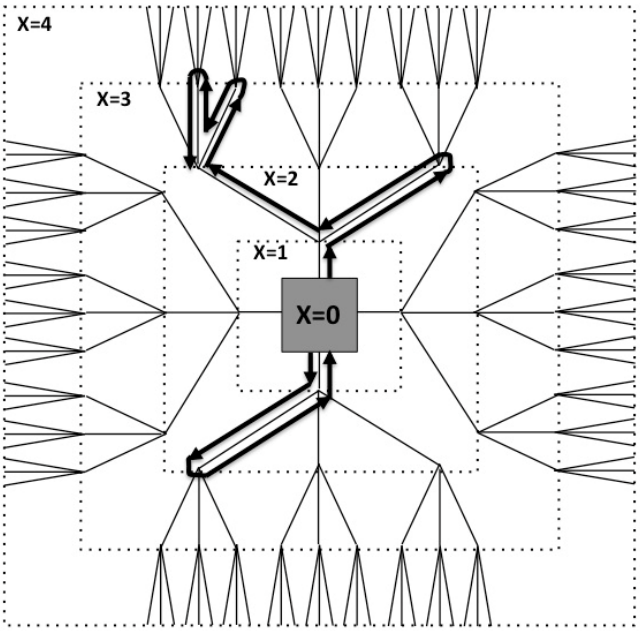

Fig.5